AAV-Mediated Lysophosphatidylcholine Acyltransferase 1 (*Lpcat1*) Gene Replacement Therapy Rescues Retinal Degeneration in *rd11* Mice

Xufeng Dai,[1] Juanjuan Han,[1] Yan Qi,[1] Hua Zhang,[1] Lue Xiang,[2] Jineng Lv,[2] Jie Li,[3] Wen-Tao Deng,[3] Bo Chang,[4] William W. Hauswirth,[3] and Ji-jing Pang[1,3]

[1]Eye Hospital, School of Ophthalmology and Optometry, Wenzhou Medical University, Wenzhou, Zhejiang, China
[2]Lab for Stem Cell & Retinal Regeneration, Division of Ophthalmic Genetics, The Eye Hospital of Wenzhou Medical University, Wenzhou, Zhejiang, China
[3]Department of Ophthalmology, University of Florida, Gainesville, Florida
[4]The Jackson Laboratory, Bar Harbor, Maine

Correspondence: Ji-jing Pang, Eye Hospital, School of Ophthalmology and Optometry, Wenzhou Medical University, Wenzhou, PR China; jpangoph@hotmail.com.

XD and JH contributed equally to the work presented here and should therefore be regarded as equivalent authors.

Submitted: November 21, 2013
Accepted: February 12, 2014

Citation: Dai X, Han J, Qi Y, et al. AAV-mediated lysophosphatidylcholine acyltransferase 1 (*Lpcat1*) gene replacement therapy rescues retinal degeneration in *rd11* mice. *Invest Ophthalmol Vis Sci*. 2014;55:1724–1734. DOI:10.1167/iovs.13-13654

Purpose. The retinal degeneration 11 (*rd11*) mouse is a newly discovered, naturally occurring animal model with early photoreceptor dysfunction and rapid rod photoreceptor degeneration followed by cone degeneration. The *rd11* mice carry a spontaneous mutation in the lysophosphatidylcholine acyltransferase 1 (*Lpcat1*) gene. Here, we evaluate whether gene replacement therapy using the fast-acting tyrosine-capsid mutant AAV8 (Y733F) can arrest retinal degeneration and restore retinal function in this model.

Methods. The AAV8 (Y733F)-smCBA-*Lpcat1* was delivered subretinally to postnatal day 14 (P14) *rd11* mice in one eye only. At 10 weeks after injection, treated *rd11* mice were examined by visually-guided behavior, electroretinography (ERG) and spectral domain optical coherence tomography (SD-OCT), and then killed for morphologic and biochemical examination.

Results. Substantial scotopic and photopic ERG signals were maintained in treated *rd11* eyes, whereas untreated eyes in the same animals showed extinguished signals. The SD-OCT (in vivo) and light microscopy (in vitro) showed a substantial preservation of the outer nuclear layer in most parts of the treated retina only. Almost wild-type LPCAT1 expression in photoreceptors with strong rod rhodopsin and M/S cone opsin staining, and normal visually-guided water maze behavioral performances were observed in treated *rd11* mice.

Conclusions. The results demonstrate that the tyrosine-capsid mutant AAV8 (Y733F) vector is effective for treating rapidly degenerating models of retinal degeneration and, moreover, is more therapeutically effective than AAV2 (Y444, 500, 730F) vector with the same promoter-cDNA payload. To our knowledge, this is the first demonstration of phenotypic rescue by gene therapy in an animal model of retinal degeneration caused by *Lpcat1* mutation.

Keywords: *rd11*, gene therapy, mice, *Lpcat1*, AAV

Inherited retinal degenerations are a group of clinically and genetically diverse conditions that result from mutations in more than 200 different genes (data available in the public domain at http://www.sph.uth.tmc.edu/Retnet). Many of the genes mainly affect the function and viability of rod and cone photoreceptors, ultimately leading to photoreceptor loss and blindness. Retinitis pigmentosa (RP) is a subset of common inherited retinal degenerations with progressive vision loss, such as nyctalopia in early stages of the disease with visual-field scotomas in advanced stages due to photoreceptor loss.[1] Thus far, over 45 genes have been linked to inherited forms of RP (Retnet; available in the public domain at www.sph.uth.tmc.edu/retnet). Currently, there is no treatment for this debilitating disorder. Mouse models of retinal degeneration have been studied for decades with the aim of exploring the causes of photoreceptor death and finding therapeutic modalities.[2]

The *rd11* mice carry a single nucleotide insertion (c.420-421insG) in exon 3 of the lysophosphatidylcholine acyltransferase-1 (*Lpcat1*) gene, which leads to premature truncation of the LPCAT1 protein.[3] As a phospholipid remodeling enzyme, LPCAT1 promotes the conversion of palmitoyl-lysophosphatidylcholine (LPC) to dipalmitoylphosphatidylcholine (DPPC).[4,5] Consistent with this, retinal lipid analysis of *rd11* retinas showed remarkably decreased DPPC levels compared to wild-type mice,[3] suggesting a causal link to photoreceptor dysfunction. The *rd11* mice exhibit rapid retinal degeneration starting at approximately postnatal day 21 (P21), and by P28 only half of the normal compliment of photoreceptor cells remains, while at P42 most photoreceptors have been lost; rod photoreceptors are affected before cones, consistent with an RP-like phenotype.[3]

In the past decade, the development of new generations of viral vectors has made it possible to deliver genes stably to retinal cells. At present, the most effective gene delivery vectors are those derived from adeno-associated virus (AAV).[6–9] At least nine AAV serotypes (AAV1–AAV9) have been evaluated for ocular use so far.[2,9] Recently, it was reported that epidermal

growth factor receptor protein tyrosine kinase (EGFR-PTK)-mediated tyrosine phosphorylation of exposed residues of the AAV capsid promotes ubiquitination and subsequent proteasomal degradation of AAV particles, which decreases AAV vector transduction efficiency.[10] Site-directed tyrosine to phenylanine (Y-F) mutagenesis of selected, surface exposed tyrosine residues in AAV2 was shown to protect vector particles from proteasomal degradation and significantly increase the transduction efficiency of these mutant AAV vectors relative to the wild-type AAV vectors.[10] Among the AAV vectors with different Y-F point mutations, AAV8 containing a single point mutation (Y733F) and AAV2 with three Y-F mutations (Y444, 500, 730F) both showed strong reporter gene expressions in photoreceptors following subretinal injection compared to wild type AAV2.[11,12] Using the AAV8 (Y733F) vector, we then successfully restored long-term vision to *rd10* mouse, a model of RP with a PDEβ mutation.[7] Here, we tested whether an AAV8-733 vector-mediating *Lpcat1* expression also is capable of preserving retinal structure and function in *rd11* mice that exhibit a rapid retinal degeneration.

Materials and Methods

Animals

The C57BL/6J mice and the congenic inbred strain of *rd11* mice were obtained from the Jackson Laboratory (Bar Harbor, ME). All mice were bred and maintained in the Animal Facilities of Wenzhou Medical University. The animals were maintained in a 12-hour light/12-hour dark cycle with an ambient light intensity of 18 lux, and with free access to food and water. All experiments were approved by Wenzhou Medical University's Institutional animal care and use committee, and were conducted in accordance with the ARVO Statement for the Use of Animals in Ophthalmic and Vision Research.

Construction of AAV Vectors

The AAV serotype 8 capsids containing a point mutation in tyrosine residue 733 changing it to a phenylalanine residue, AAV8 (Y733F), was used for packaging the vector DNA. For purposes of retinal rescue comparison, the vector also was packaged in AAV2 (Y444, 500, 730F) capsids. Vector plasmids were constructed by cloning mouse *Lpcat1* cDNA[3] under the control of the ubiquitous, constitutive smCBA promoter[7,13] to generate pTR-smCBA-*Lpcat1*. The AAV vectors were packaged and purified at University of Florida according to previously reported methods.[14]

Subretinal Injections

At P14, 1 μL of AAV8 (Y733F)-smCBA-*Lpcat1* (10^{13} vector genomes per mL) was injected subretinally into one eye of *rd11* mice. Subsets of mice also were injected in one eye only with equal volumes and concentrations of AAV2 (Y444, 500, 730F)-smCBA-*Lpcat1*. All partner eyes remained uninjected. Subretinal injections were performed as described previously.[15] Only animals with no apparent surgical complications, and their initial retinal blebs occupied >50% of the retinal area, were retained for further evaluation. A total of 20 *rd11* mice met this criterion, which resulted in at least three animals for each experiment. Following all injections, 1% atropine eye drops, and tetracycline and cortisone acetate eye ointments were given.

Electroretinography (ERG)

At 4, 7, and 10 weeks following subretinal injection, a RETIport system with a custom-built Ganzfeld dome (Roland Consult, Wiesbaden, Germany) was used for electroretinographic recording as described previously,[6,8] with minor modifications. Dark-adapted ERGs were recorded at −1.85 and 0 log cd-s/m^2 stimulus intensity with an interstimulus interval of 30 seconds; 5 ERG scans were averaged for dark-adapted ERGs. Light-adapted ERGs were elicited after a steady background illumination of 30 cd/m^2 presented for 10 minutes. Then, 50 signals were averaged for photopic measurements taken at 0.65 log cd-s/m^2 in background light with an interstimulus interval of 0.4 seconds. Ganzfeld illumination with white light stimulus was applied for a duration of 2 milliseconds. B-wave amplitudes were defined as the difference between the trough and peak of each waveform. Scotopic and photopic b-wave amplitudes from untreated, treated *rd11*, and uninjected normal C57BL/6J eyes were averaged.

Spectral Domain Optical Coherence Tomography (SD-OCT) Imaging

At 7 and 10 weeks posttreatment, pupils of AAV8 (Y733F)-smCBA-*Lpcat1*–treated and untreated *rd11* eyes were dilated with 1% atropine and 2.5% phenylephrine hydrochloride. Mice then were anesthetized as described previously.[6] One drop of 2.5% hydroxypropyl methylcellulose was administrated to eyes before examination. The SD-OCT was performed using a machine manufactured by Bioptigen (Durham, NC). Three lateral images (nasal to temporal) were collected, starting 0.4 mm above the meridian crossing through the center of the optic nerve (ON), at the ON meridian, and 0.4 mm below the ON meridian. A corresponding box centered on the ON with eight measurement points separated by 0.4 mm from each other was created with the similar methods described previously.[7] Corresponding neural retina thicknesses for untreated, treated *rd11,* and uninjected normal C57BL/6J eyes were compared at the same location (0.4 mm temporal to the ON) by measuring the distance from the vitreal face of the ganglion cell layer to the apical face of the retinal pigment epithelium.

Histology

Following SD-OCT examination, eyes were enucleated and eyecups were prepared for light microscopic examination. Structural evaluation was done as described previously with some modifications.[7,16] Briefly, eyes were fixed in 4% paraformaldehyde solution and embedded in paraffin. Sections (4 μm thick) were stained with hematoxylin and eosin before photographing with a Zeiss bright-field microscope (BX41; Olympus, Tokyo, Japan) fitted with Windows version 4.6 spot software. Images of the posterior pole were collected. Corresponding neural retina thicknesses for untreated, treated *rd11*, and uninjected normal C57BL/6J eyes were compared at the edge of the optic disc by measuring the distance from the vitreal face of the ganglion cell layer to the apical face of the retinal pigment epithelium.

Immunocytochemistry

Eyes from AAV8 (Y733F)-smCBA-*Lpcat1*–treated and untreated *rd11* mice, along with age-matched C57BL/6J mice, were enucleated and the eyecups were processed as described previously, with some modifications.[17,18] Briefly, after enucleation, eyes were fixed in fresh 4% paraformaldehyde in 0.1 M phosphate buffer (pH 7.4) overnight at 4°C. After fixation, the cornea, lens, and vitreous were removed to generate eye cups. Retinal whole mount preparations were generated by first removing the ON head and then carefully separating the neuroretina from the eye cup. Alternatively, frozen sections (10

Investigative Ophthalmology & Visual Science

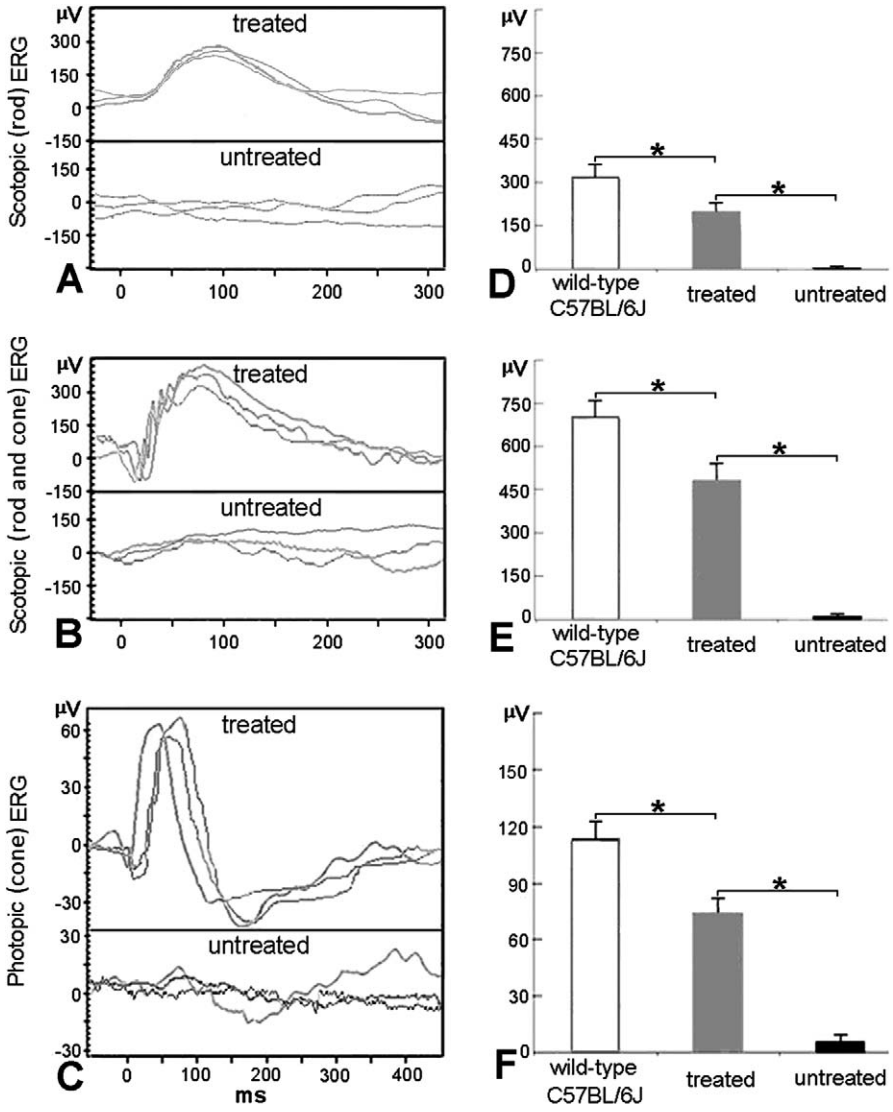

Figure 1. Scotopic and photopic ERGs in treated and untreated *rd11* eyes. (**A**) Representative scotopic (rod) ERG elicited from −1.85 log cd-s/m^2 flash intensity in three *rd11* eyes 10 weeks following treatment at P14 (*upper row*) compared to those of the untreated eyes (*lower row*) from the same *rd11* mice. (**B**) Representative scotopic (rod and cone) ERG elicited from 0 log cd-s/m^2 flash intensity in three *rd11* eyes 10 weeks following treatment at P14 (*upper row*) compared to those of the untreated eyes (*lower row*) from the same *rd11* mice. (**C**) Representative photopic (cone) ERG elicited at 0.65 log cd-s/m^2 flash intensity from the same *rd11* mice (*upper row*, treated; *lower row*, untreated). (**D**) Average scotopic (rod) b-wave amplitudes elicited at −1.85 log cd-s/m^2 intensity in age-matched, uninjected wild-type C57BL/6J, AAV8 (Y733F) treated and untreated *rd11* eyes. (**E**) Average scotopic (rod and cone) b-wave amplitudes elicited at 0 log cd-s/m^2 intensity in age-matched, uninjected wild-type C57BL/6J, AAV8 (Y733F) treated and untreated *rd11* eyes. (**F**) Averaged photopic (cone) b-wave amplitudes elicited at 0.65 log cd-s/m^2 intensity in age-matched, uninjected normal C57BL/6J, AAV8 (Y733F) treated and untreated *rd11* eyes. *$P < 0.05$.

Table. Statistical Comparison of the Scotopic and Photopic B-Wave Amplitudes of WT, Treated (P14+10W), and Untreated *rd11* Mice

		***rd11* Mice**		***P* Value**		
Amplitude of b-Wave, μV	**WT Mice**	**Treated**	**Untreated**	**Treated vs. Untreated**	**WT vs. Treated**	**WT vs. Untreated**
Scotopic (rod) ERG	317.0 ± 40.9	202.7 ± 32.2	3.0 ± 5.2	<0.001*	0.004†	<0.001*
Scotopic (rod and cone) ERG	705.7 ± 61.5	479.3 ± 58.0	9.7 ± 9.5	<0.001*	0.001†	<0.001*
Photopic (cone) ERG	114.3 ± 9.0	75.3 ± 7.5	4.7 ± 4.5	<0.001*	0.001†	<0.001*

In uninjected normal C57BL/6J, treated, and untreated *rd11* eyes, the average rod-driven b-wave amplitudes showed significant differences by 1-way ANOVA ($F = 83.190$, $df = 2$, $P < 0.001$). The maximum mixed responses of rods and cones showed significant differences ($F = 156.634$, $df = 2$, $P < 0.001$). The averages of light-adapted ERG amplitudes also showed significant differences ($F = 176.027$, $df = 2$, $P < 0.001$). *P* values of least significant difference (LSD) post hoc test were calculated as above. Mean ± SD, $n = 3$/cohort.

* $P < 0.001$.

† $P < 0.05$.

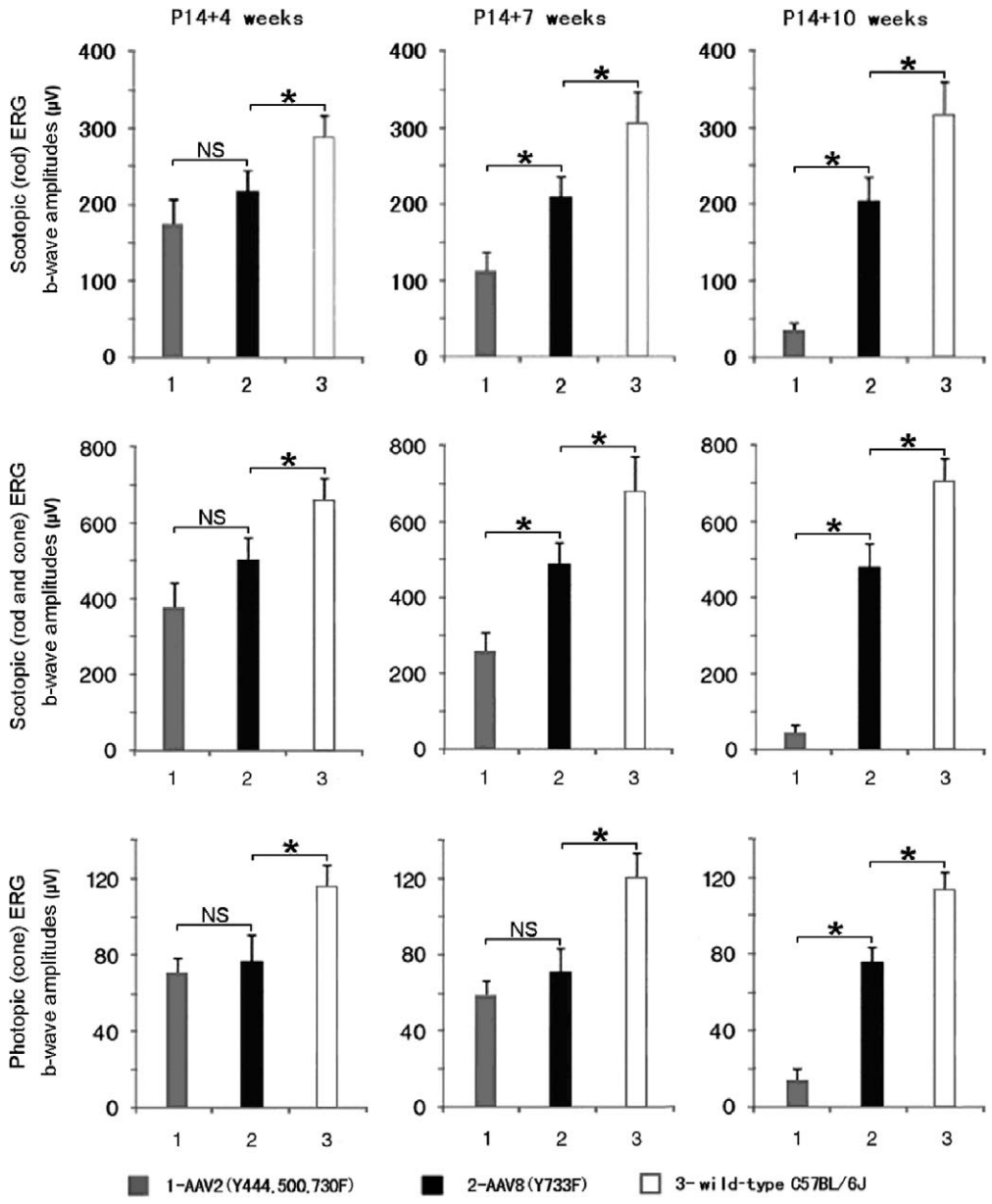

Figure 2. Comparisons of retinal function at different time points following AAV2 (Y444, 500, 730F) or AAV8 (Y733F) treatment ($n = 3$). Scotopic (rod) response is elicited at −1.85 log cd-s/m^2 flash intensity (*upper row*), while rod and cone response elicited at 0 log cd-s/m^2 (*middle row*). Photopic (cone) response is elicited at 0.65 log cd-s/m^2 (*lower row*). Only AAV8 (Y733F) mediates a rescue effect 10 weeks following P14 treatment in scotopic and photopic conditions (*right column*). *$P < 0.05$; NS, nonsignificant.

μm thick) were prepared from eye cups protected in 30% sucrose and embedded in optimal cutting temperature compound. Following permeation with 0.1% Triton X-100, sections were rinsed in 0.1 M PBS, blocked in 5% bovine serum albumin (BSA), then incubated overnight at 4°C in rabbit anti-mouse LPCAT1 antibodies (1:750, HPA022268; Sigma-Aldrich, St. Louis, MO). After 3 rinses with 0.1 M PBS, sections were incubated in goat anti-rabbit IgG conjugated to Cy3 fluorochrome (1:400, AP187C; Merck Millipore, Darmstadt, Germany) for 2 hours followed by 3 rinses with 0.1 M PBS. Sections then were mounted with coverslips before fluorescence photography. Retinal whole mounts and frozen sections were prepared for M/S-cone opsin[18] or rod rhodopsin[19] antibody staining according to previously described methods.

Western Blot Analysis

Western blot was performed as described previously.[15] Retinas were dissected carefully from treated and untreated *rd11* eyes, and normal C57BL/6J eyes. Protein was extracted using the RIPA method, quantified by a BCA protein assay kit (Beytime, Jiangsu, China), separated by SDS-PAGE, and then transferred to a PVDF membrane. The membranes were incubated with anti-LPCAT1 polyclonal antibody (Sigma, Shanghai, China) overnight at 4°C. Anti-rabbit HRP-conjugated secondary antibodies (Cell Signaling, Shanghai, China) were used to detect the primary antibody. Rabbit anti-GAPDH monoclonal antibody (Cell Signaling) was used as an internal loading control.

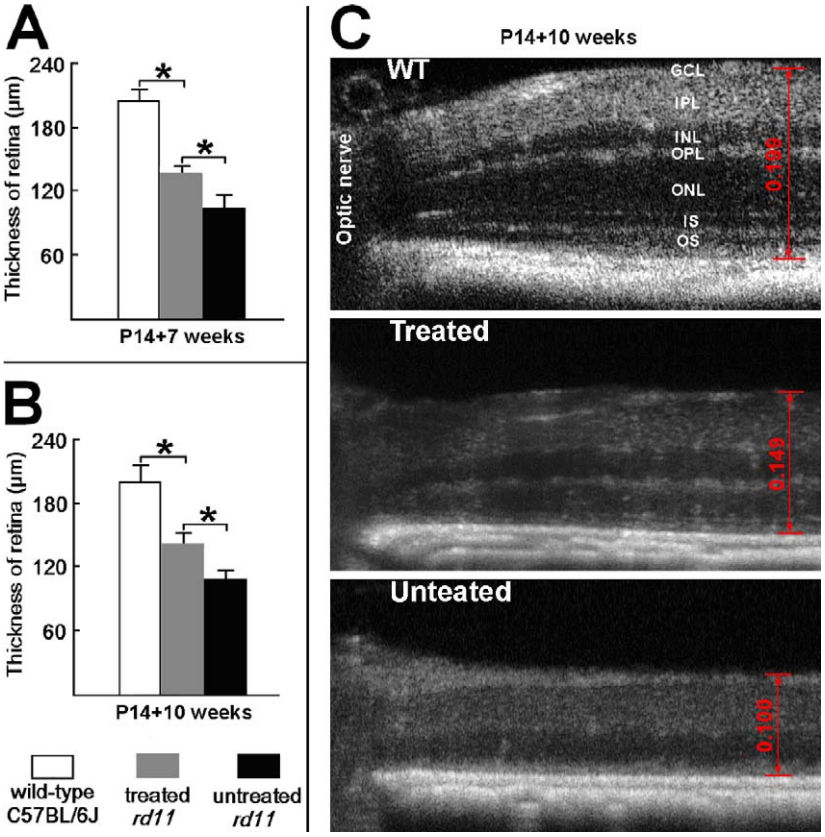

Figure 3. The SD-OCT of AAV8 (Y733F)-treated and untreated eyes from *rd11* mouse. The OCT images show the retinal thickness at same location (0.4 mm temporal to the optic nerve). (**A**) At 7 weeks after P14 treatment, averaged retinal thicknesses in age-matched, uninjected normal C57BL/6J, treated, and untreated *rd11* eyes ($n = 3$). (**B**) At 10 weeks after P14 treatment, averaged retinal thicknesses in wild-type, treated, and untreated *rd11* eyes ($n = 3$). (**C**) The OCT images (10 weeks after P14 treatment) at same location from representative wild-type, treated, and untreated *rd11* eyes. *Scale calipers* on each image are placed at equivalent distances from the optic nerve to quantify the distance from the vitreal face of the ganglion cell layer to the apical face of the RPE (0.149 mm for a treated, 0.100 mm for the partner untreated *rd11* eye, and 0.199 mm for a wild-type C57BL/6J eye). *$P < 0.05$. OS, outer segments; IS, inner segments; OPL, outer plexiform layer; INL, inner nuclear layer; IPL, inner pexiform layer; RGC, retinal ganglion cell.

Visually-Guided Behavioral Test

The water maze visually-guided behavioral test has been described previously.[20] Briefly, 10 weeks after injection, AAV8 (Y733F)-smCBA-*Lpcat1*–treated *rd11* mice, together with age-matched untreated *rd11* and normal C57BL/6J mice, were trained initially in a plastic water tank with a platform positioned in a well-lit room (18 lux) followed by formal training under the same photopic conditions. Formal training consisted of three blocks of four trials per day for 4 consecutive days. During each trial, the mouse was placed in the water from one of four equally spaced start locations. Behavioral data were acquired as the latency to escape to the platform during the training trials. Subjects were given up to 60 seconds to escape during each trial. If they did not escape within the allotted time, they were guided gently to the platform and their escape time was recorded as 60 seconds. The mice then were tested in scotopic condition with very dim light (not detectable with the Datalogging Light Meter, model 401036; Extech Instruments, Waltham, MA). One day following the performance in dim light, the treated eye of each *rd11* mouse was sutured. The next day, the water maze tests were repeated in dim light and well-lit environments.

Statistical Analysis

Data were presented as mean ± SD. SPSS 18.0 (IBM Corporation, Armonk, NY) was used for statistical analysis. Paired sample *t*-test or 1-way ANOVA with least significant difference (LSD) post hoc test was used for comparison between two groups and among three groups for measurement data. Differences were defined as significant at $P < 0.05$.

Results

AAV8 (Y733F) Rescues Retinal Function (ERG) in the *rd11* Mouse for at Least 10 Weeks

At 10 weeks after treatment with AAV8 (Y733F)-smCBA-*Lpcat1*, *rd11* mice were examined by scotopic and photopic ERGs. Rescue of dark-adapted (Figs. 1A, 1B) and light-adapted (Fig. 1C) ERG responses were observed and maintained in treated *rd11* eyes, whereas ERG responses were nearly extinguished in untreated *rd11* eyes. The b-wave amplitudes were significantly improved in treated *rd11* eyes ($P < 0.05$) to levels approximately two-thirds of that in normal age-matched uninjected C57BL/6J control mice ($P < 0.05$, Figs. 1D–F, $n = 3$). The b-wave amplitudes and statistical comparisons of these measurements were shown in the Table. To measure the sensitivity of the rod and cone systems in the treated eyes, we analyzed the implicit time of the relevant b-waves. Independent samples *t*-test was used to detect differences in the treated *rd11*and uninjected normal C57BL/6J retina. No significant difference was found in implicit times of the rod-derived b-waves between the treated *rd11* eyes (91.3 ± 5.7 ms) and

Investigative Ophthalmology & Visual Science

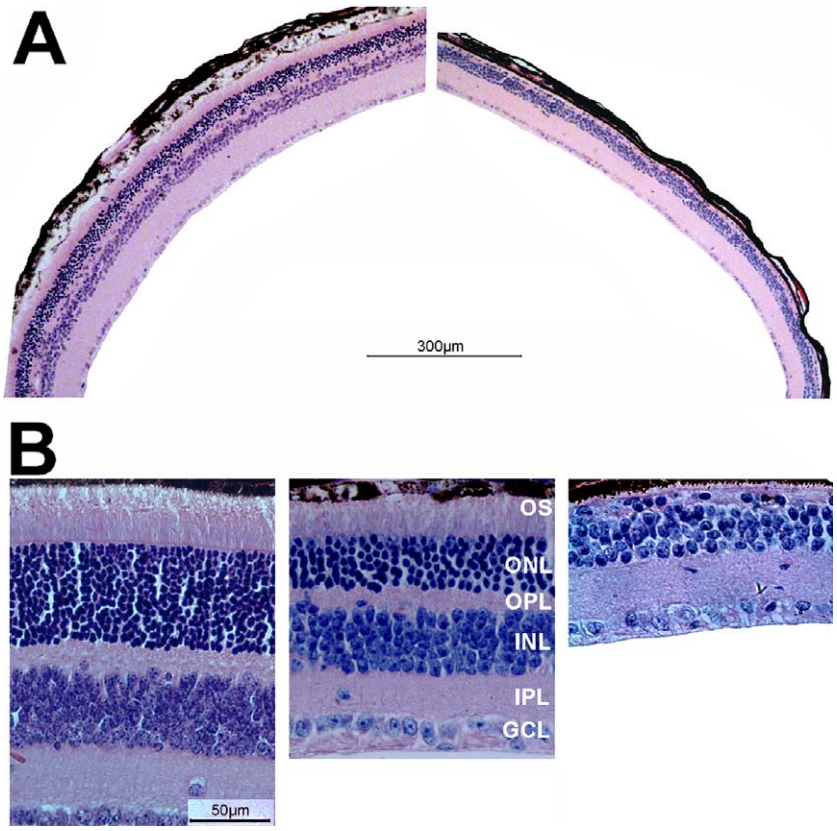

FIGURE 4. Light microscopic images of treated and untreated retinal sections from *rd11* and normal mice. (**A**) Low-magnification images from the treated (*left*) and untreated (*right*) eyes of the same *rd11* mouse 10 weeks after P14 treatment. Note the presence of outer segments and a continuous, intact ONL in the treated eye, and its absence in the untreated eye. (**B**) Higher magnification images from a 3-month old uninjected normal C57BL/6J eye (*left*), the treated (*middle*), and untreated (*right*) eyes of the same *rd11* mouse.

C57BL/6J eyes (93.0 ± 5.6 ms, $n = 3$, $t = -0.363$, $P = 0.735$). No significant difference in maximum combined response was found between the treated *rd11* eyes (75.3 ± 4.5 ms) and C57BL/6J eyes (74.7 ± 5.0 ms, $n = 3$, $t = 0.171$, $P = 0.873$). Furthermore, no statistical difference was found in implicit times of the cone-derived b-waves between the treated *rd11* (58.3 ± 6.5 ms) and C57BL/6J eyes (55.0 ± 5.0 ms, $n = 3$, $t = 0.704$, $P = 0.520$).

To compare the effectiveness between AAV8 (Y733F)– and AAV2 (Y444, 500, 730F)–mediated treatments, we analyzed scotopic and photopic ERG amplitudes in mice injected at P14 with each vector at 4, 7, and 10 weeks after treatment (Fig. 2). At 4 weeks after treatment, scotopic and photopic ERG responses were higher in *rd11* eyes treated with AAV8 (Y733F)-smCBA-*Lpcat1* than those treated with AAV2 (Y444, 500, 730F)-smCBA-*Lpcat1* (Fig. 2, left column). At 7 weeks after treatment, both responses were decreased in AAV2 (Y444, 500, 730F)–treated *rd11* eyes (Fig. 2, middle column). By 10 weeks after treatment, scotopic and photopic ERGs were almost lost in AAV2 (Y444, 500, 730F)–treated *rd11* eyes, while AAV8 (Y733F)–mediated ERG amplitude gains remained stable (Fig. 2, right column).

AAV8 (Y733F)-smCBA-*Lpcat1* Treatment Preserves Retinal Structure in *rd11* Eyes

The SD-OCT allows in vivo assessment of retinal thickness in treated versus untreated eyes. At 7 and 10 weeks after treatment, OCT examinations were carried out on AAV8 (Y733F)–treated and untreated *rd11* eyes. To compare structural differences, retinal thickness was measured carefully at the same location (0.4 mm temporal to the optic nerve) in all eyes analyzed (Fig. 3). At 10 weeks following treatment, significant differences were found in retinal thickness among the untreated, treated *rd11*, and uninjected normal C57BL/6J mice (0.108 ± 0.008, 0.141 ± 0.010, and 0.199 ± 0.015 mm, respectively, 1-way ANOVA, $F = 52.456$, $df = 2$, $P < 0.001$). The LSD analysis revealed a statistical difference between the untreated and treated *rd11* retina ($P = 0.01$), and a significant difference between treated *rd11* and normal uninjected C57BL/6J retina ($P = 0.001$).

Following OCT examination at 10 weeks after treatment, *rd11* mice were sacrificed and eyes enucleated for histology. Hematoxylin and eosin staining of AAV8 (Y733F)-smCBA-*Lpcat1*–treated and contralateral, untreated controls *rd11* retinas confirmed OCT results. Using a retina from a representative *rd11* mouse that received >90% retinal detachment after injection; that is, had a large area of retina exposed to the vector, light microscopy at low-magnification revealed a relatively normal outer nuclear layer (ONL) throughout the retina (Fig. 4A, left). In contrast, it was difficult to visualize any ONL in the untreated eye of the same *rd11* mouse (Fig. 4B, right). Higher-magnification images showed that approximately 2/3 of the normal outer segment length and ONL thickness were maintained in the treated *rd11* retinas compared to a normal uninjected C57BL/6J retinas (Fig. 4B, left and middle). Meanwhile, there was only one incomplete layer of nuclei in the ONL of the untreated eye from the same *rd11* mouse (Fig. 4B, right). In addition, the outer plexiform layer also became thinner in the untreated *rd11* retina (Fig. 4B,

Investigative Ophthalmology & Visual Science

right) relative to that seen in the partner-treated eye (Fig. 4B, middle). Significant differences were found in retinal thickness among the untreated, treated *rd11*, and uninjected normal C57BL/6J mice: 0.099 ± 0.007, 0.151 ± 0.016, and 0.213 ± 0.017 mm, respectively, 1-way ANOVA, $F = 48.652$, $df = 2$, $P < 0.001$. The LSD analysis revealed a statistical difference between the untreated and treated *rd11* retina ($P = 0.004$), and a similar significant difference also was found between treated *rd11* and normal uninjected C57BL/6J retina ($P = 0.002$).

Rhodopsin and LPCAT1 Expressions Are Restored in Treated *rd11* Mice

At 10 weeks after treatment, LPCAT1, rod rhodopsin, and cone opsin expressions were assayed by immunohistochemistry from treated and untreated retinal sections of *rd11* mice. The LPCAT1 (Fig. 5A) and rod rhodopsin (Fig. 5C) staining is detected in the photoreceptor of a treated *rd11* retina, similar to the expression seen in the wild type retina, while no LPCAT1, rod rhodopsin, or cone opsin expression was observed in the partner untreated retina from the same *rd11* mouse.

Western blot analysis (Fig. 5B) showed the expression of LPCAT1 protein in treated *rd11* eyes, but not in untreated contralateral eyes. The expression level of LPCAT1 in treated *rd11* eyes was similar to that in C57BL/6J eyes.

Cone Opsin Expressions Are Restored in Treated *rd11* Mice

Early and rapid cone degeneration with cone opsin loss has been reported in *rd11* mice.[3] To examine whether the cone opsins are preserved 10 weeks after P14 treatment, retinal whole mounts and frozen sections were stained with cone opsin–specific antibodies. Using retinal whole mounts from *rd11* mice that received >90% retinal detachment, fluorescent microscopy at low magnification revealed that M-opsins were preserved in the dorsal and ventral hemispheres of the retina (Fig. 6, middle row), while little M-opsin remained in any portion of the untreated *rd11* retina (Fig. 6, bottom row). High-magnification images showed that the M-opsin distribution pattern in treated *rd11* retina (Fig. 6, left 2 columns, middle row) was similar to that of the normal C57BL/6J retina (Fig. 6, left 2 columns, upper row). In frozen section, strong M-opsin staining is evident in the outer segments of the treated *rd11* retina (Fig. 6, right 2 columns, middle row), which was similar to that in a normal C57BL/6J retina (Fig. 6, right 2 columns, upper row). In contrast, no M-opsin expression was observed in the partner untreated eye (Fig. 6, right 2 columns, bottom row) from the same *rd11* mouse at this age. Furthermore, S-opsins also were evident in the retinal whole mounts and sections of a treated *rd11* eye with normal distribution patterns, similar to that seen in a normal C57BL/6J retina (Fig. 7).

AAV8 (Y733F) Rescues Visually-Guided Behavior in the *rd11* Mouse

To determine whether the observed electrophysiologic, biochemical, and structural preservation of the *rd11* retina following AAV8 (Y733F) vector treatment led to improvement in behavioral performance, we tested the mice in a visually-guided water maze task with our described previously method.[20] After preliminary training,[20] times to escape to the platform under room light conditions were recorded. Among three groups, average times to find the platform showed

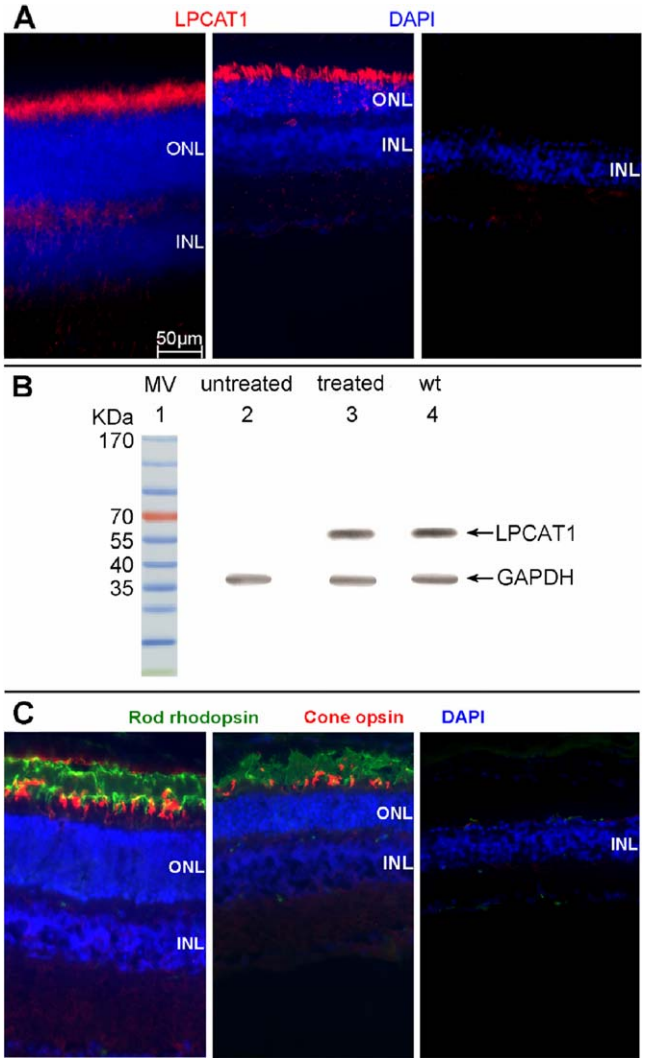

Figure 5. The LPCAT1, rod rhodopsin and cone opsin expression in treated and untreated eyes of *rd11* mice. (**A**) LPCAT1 immunostaining (*red*) in a 3-month old uninjected normal C57BL/6J eye (*left*), treated (*middle*), and untreated eye (*right*) from the same *rd11* mouse. (**B**) Western blot showing the expression of LPCAT1 from AAV8 (Y733F)-smCBA-*Lpcat1*–treated and untreated *rd11* eyes, and untreated age-matched normal C57BL/6J normal eyes ($n = 3$). *Lane 1*: molecular weight marker. *Lane 2*: untreated *rd11* retina. *Lane 3*: treated *rd11* retina. *Lane 4*: normal C57BL/6J retina. (**C**) Double staining of rod rhodopsin (*green*) and cone opsin (*red*) in a 3-month old uninjected normal C57BL/6J eye (*left*), treated (*middle*), and untreated eye (*right*) from the same *rd11* mouse. Nuclei were stained with DAPI (*blue*). Note the robust staining of LPCAT1, rod rhodopsin and cone opsin in the treated *rd11* eye compared to its absence in the untreated, contralateral control eye.

significant differences by 1-way ANOVA ($F = 22.688$, $df = 3$, $P < 0.001$). The normal C57BL/6J mice took 7.7 ± 1.1 seconds, the treated *rd11* mice took 15.3 ± 3.3 seconds, and untreated *rd11* mice took 49.6 ± 9.4 seconds to reach the platform. Statistical analysis showed significant improvement in treated *rd11* mice compared to untreated *rd11* mice ($n = 3$, $P < 0.001$). No statistical difference of performance was found between treated *rd11* and normal C57BL/6 mice ($P = 0.267$).

In addition, when we closed the treated eyes by suturing their eyelids, time to reach the platform increased from 15.3 ± 3.3 to 43.7 ± 14.2 seconds. No statistical difference of performance was found between untreated *rd11* mice and

Investigative Ophthalmology & Visual Science

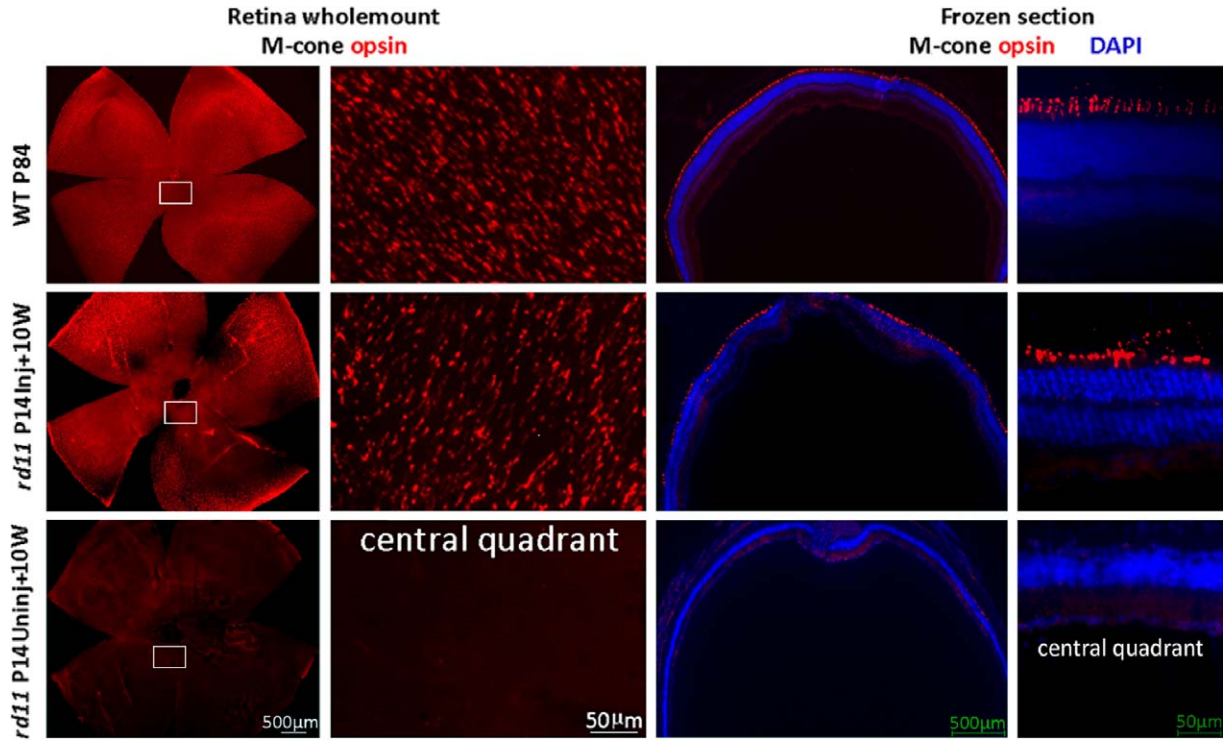

Figure 6. M-cone opsin preservation in treated *rd11* retinas. At 10 weeks after P14 treatment, staining of M-opsins in retinal whole mounts (*left two columns*) revealed a pattern of M-opsin–containing cones in treated *rd11* retinas (right eyes) compared to those from C57BL/6J eyes (left eyes). In the contralateral uninjected left eyes, little M-opsin-positive cells are seen. Frozen sections (*right two columns*) showed that the preserved M-cone opsin is located in photoreceptor outer segments in normal C57BL/6J and treated *rd11* retinas. *Red*: M-cone opsin staining. *Blue*: DAPI (4′,6-diamidino-2-phenylindole) stained nuclei. P, postnatal day; Inj, injected; Uninj, uninjected; W, weeks.

treated *rd11* mice when the treated eyes were sutured ($P = 0.656$).

Analysis of times to escape to the platform under very dim light conditions (Fig. 8B) showed similar results as those from room light conditions (Fig. 8A). The normal C57BL/6J mice took 8.5 ± 1.3 seconds, *rd11* mice with one eye treated took 15.4 ± 3.4 seconds, and untreated *rd11* mice took 41.8 ± 6.4 seconds to reach the platform. When the treated eyes of *rd11* mice were sutured, time to reach the platform increased to 46.7 ± 16.5 seconds. Statistical comparisons between groups were shown in Figure 8B.

Discussion

To our knowledge, this study is the first demonstration that restoration of retinal function and structure can be achieved in the *rd11* mouse following gene replacement therapy. It further confirmed that retinal degeneration in *rd11* mice is caused by *Lpcat1* gene mutation. In addition, for the first time, we provided evidence that AAV8 (Y733F) vector has higher therapeutic efficiency than AAV2 (Y444, 500, 730F) in rod and cone photoreceptors in which the visual signal originates.

The *rd11* mice showed an early onset, rapid retinal degeneration starting at approximately P21. In this study, we treated at P14, the earliest age we can perform successful transcorneal subretinal injection. Vector injected earlier than P14 does induce transgene expression earlier; however, it is difficult to detach a significant fraction of the mouse retina before eye opening at P14, and surgical manipulation at this early stage can cause substantial injection-related damage.[15,18,21] Although sufficient transgene expression in the target cells before irreversible cell loss clearly is essential for effective rescue, it does not necessarily follow that the earlier, the better for subretinal injection-related gene replacement therapy. We have noted that the optimal stable rescue is related to the extent of retinal coverage by the vector and might be offset by injection-related damage. For example, P14 treatment[15] was more therapeutically effective than P2 treatment in the rapid degenerating *rd10* mouse, since P14 injection can transfect almost 100% of the retina with less injection-related damage, while less retinal coverage and more injection-related damage can be caused by an early P2 subretinal injection.[22] Additionally, we noted that it is difficult to arrest photoreceptor degeneration in the *rd11* mouse if treatment initiates later than P14 (data not shown). A plausible explanation is that the retinal degeneration starts before P21 when a clear photoreceptor loss is observed in *rd11* mice in addition to the fact that it takes at least several days for sufficient vector gene expression to alter photoreceptor fate. Therefore, the solid therapeutic outcome achieved by our approach may derive from a combination of optimizing the area of vector exposure, minimizing injection-related damage, and selecting an optimal treatment age.

Vectors based on AAV2 have been used extensively in many retinal gene-delivery applications, including several successful clinical trials for one type of Leber congenital amaurosis with mutant gene in retinal pigment epithelial (RPE) cells.[23–25] Many studies have focused on improving AAV2 transduction efficiency and cellular specificity by genetically engineering its capsid.[10,12,26,27] Capsid surface tyrosine mutations in AAV2 and AAV8 displayed significantly enhanced transduction efficiency in the retina compared to their wild-type counterparts.[11] Among them, AAV2 (Y444, 500, 730F) and AAV8 (Y733F)

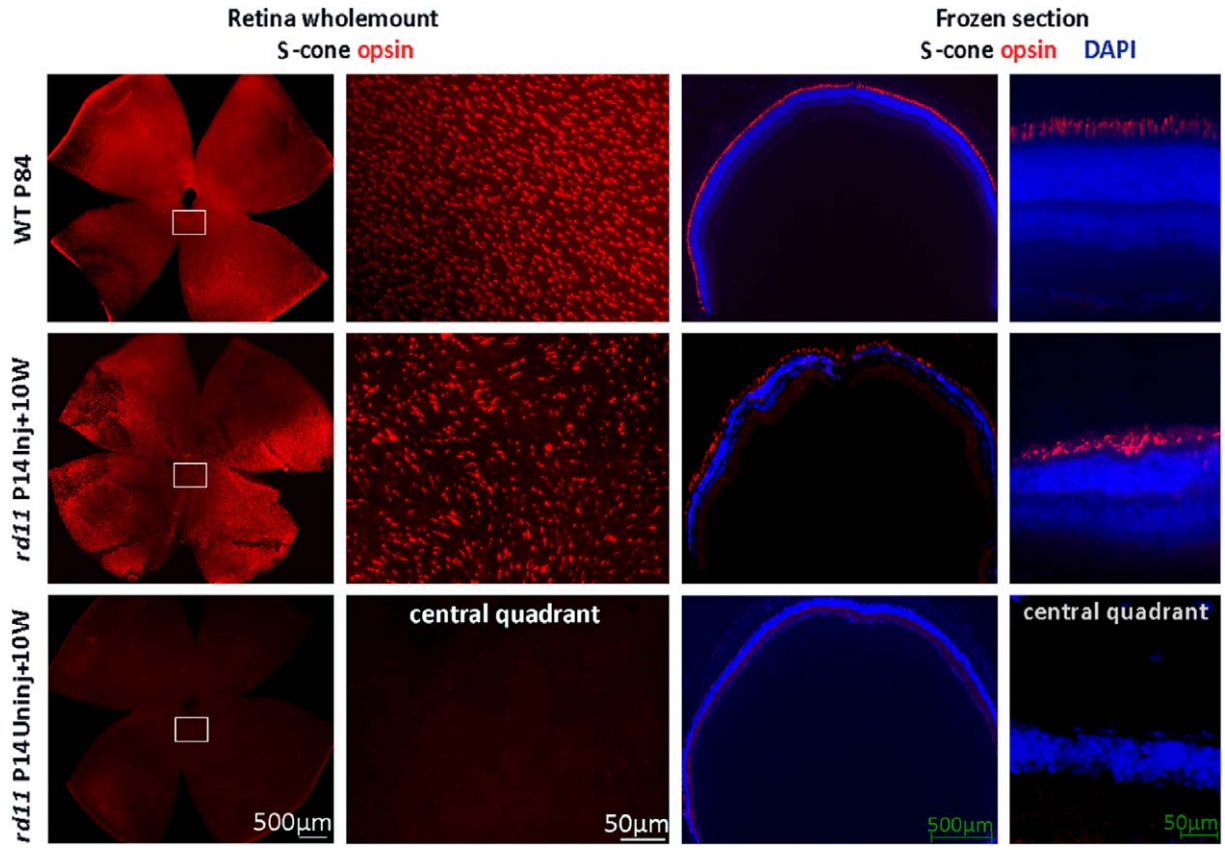

Figure 7. S-cone opsin preservation in treated *rd11* retinas. At 10 weeks after P14 treatment, staining of S-cone opsins in retinal whole mounts (*left two columns*) revealed patterns of S-opsin–containing cones in treated *rd11* eye similar to that from C57BL/6J eye. In the contralateral uninjected left eye, no S-cone opsin-positive cells were apparent. Frozen sections (*right two columns*) showed that the preserved S-opsin is located in photoreceptor outer segments in normal C57BL/6J and treated *rd11* retinas. *Red*: S-cone opsin staining. *Blue*: DAPI (4′,6-diamidino-2-phenylindole) stained nuclei.

showed robust reporter gene expression in photoreceptor cells following subretinal injections.[11,12]

Our ERG results (Fig. 2) showed that rod- and cone-mediated function were nearly lost 10 weeks after AAV2 (Y444, 500, 730F) treatment, but remained stable after AAV8 (Y733F) treatment. From our experience, AAV5 mediated photoreceptor gene therapy is more effective than that of AAV2, and that for AAV8 is the highest.[7,20] It is possible that the slower onset of transgene expression mediated by AAV2 (Y444, 500, 730F) is the cause of the difference. This result highlights the need for careful consideration of vector serotype in any therapeutic AAV vector platform. Similar to that seen with AAV8 (Y733F)–mediated responses, rod and cone responses in AAV2 (Y444, 500, 730F)–treated mice reached their maximum level of improvement at 4 weeks after treatment (Fig. 2). However, full-field ERG amplitudes decreased progressively after that time point despite early treatment. At 7 weeks after treatment, AAV2 (Y444, 500, 730F)–mediated responses (Fig. 2) showed cone responses decreased approximately 15%, whereas rod responses decreased approximately 35%, compared to those at 4 weeks. Meanwhile, rod- and cone-mediated retinal functions were stable for at least 10 weeks in AAV8 (Y733F)–treated eyes. Because cones are responsible primarily for useful daytime vision in humans, rescuing cone photoreceptors is an essential component for any successful treatment for retinal degeneration. Unlike the human retina, in which the density of cones is very high in the central macula (fovea), M- and S-cone distributions in the mouse retina are relatively even, although there are more M-cones in superior (dorsal) retina and more S-cones in inferior (ventral) retina in mice. Currently, the most reliable way to evaluate successful cone rescue in the mouse is to analyze those treated eyes in which subretinal vector had detached almost the entire retina and, thus, treated the maximum fraction of cones. We found 1 μL of subretinal vector to be sufficient to achieve almost 100% of detachment that resulted in a homogenous shallow bleb, which resolved earlier and appeared to minimize subsequent retinal detachment–related photoreceptor loss (data not shown). From our previous work on cone therapy in *rd12* (mutant *Rpe65*) mouse, we found that a single subretinal injection of AAV-*Rpe65* at P14 can restore cone ERG amplitudes to approximately 2/3 of wild type levels,[20] similar to that reported here. This is consistent with M- and S-cone degeneration being prevented for at least 10 weeks in *rd11* retinas.

Visually-guided water maze task has been used in dim light condition to test the AAV-mediated rod function restoration in *rd12* mice that have no rod function at all.[20] Here, we extended the application to test the cone-related function in photopic condition in *rd11* mice.

Our data showed clearly that electrophysiologic, biochemical, and structural preservation/restoration following AAV8 (Y733F) vector treatment also led to improvements of rod and cone vision in *rd11* mice.

The LPCAT1 is a phospholipid biosynthesis/remodeling enzyme catalyzing conversion of palmitoyl LPC to DPPC, an important lipid component of cell membrane. The loss of

Investigative Ophthalmology & Visual Science

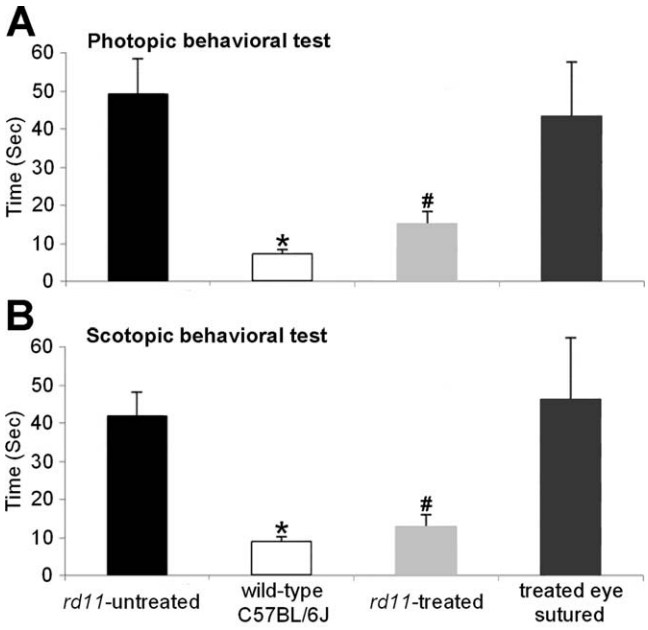

Figure 8. Water maze visually-guided behavioral test of 3-month-old uninjected normal C57BL/6J mice, treated and untreated *rd11* mice, and treated *rd11* mice with the treated eye sutured. In photopic (**A**) and scotopic (**B**) conditions: *Statistical analysis indicates a significant difference of performance ($P < 0.001$) in the normal C57BL/6 mice, compared to untreated *rd11* mice and the treated *rd11* mice when the treated eye was sutured. #Statistical analysis also indicates significant difference of performance ([**A**] $P = 0.001$, [**B**] $P < 0.001$) in the treated *rd11* mice, compared to the untreated *rd11* mice and the treated *rd11* mice with the treated eye sutured. No statistical difference of performance was found between treated *rd11* and normal C57BL/6J mice ([**A**] $P = 0.267$, [**B**] $P = 0.051$) or between untreated *rd11* mice and treated *rd11* mice when the treated eye was sutured ([**A**] $P = 0.656$, $P = 0.143$). *Columns* and *bars* represent mean ± SD ($n = 3$).

LPCAT1 leads to reduced DPPC levels that, in turn, can lead to membrane disruption[28] and Ca^{2+} influx,[29] which ultimately may contribute to photoreceptor cell death. It is reported that *Lpcat1* expression is increased from P2 to P25 during retinal development.[30] Overexpression of LPCAT1 also is found in prostate cancer, colorectal cancer, and hepatoma.[31–33] Although our results showed no overexpressed LPCAT1 in treated *rd11* eyes (Fig. 5B) with no detectable tumors in treated *rd11* eyes or other organs (data not shown) in this short-term study, it is necessary to follow up this issue in the long-term evaluation.

Respiratory distress syndrome (RDS), which is the leading cause of death in premature infants, is caused by surfactant deficiency. The most critical and abundant phospholipid in pulmonary surfactant is saturated phosphatidylcholine (SatPC). The LPCAT1 is related with the synthesis of SatPC in mouse alveolar type II cells and is essential for the transition to air breathing.[34] Our AAV-*Lpcat1* gene therapy data shown here in the retina might suggest its use for therapeutic interventions in surfactant-associated deficiencies.

In this study, we demonstrated that the rapid onset and high transduction efficiency of AAV8 (Y733F) vector led to significant restoration of retinal electrophysiology, vision-guided behavioral performance, and preservation of structure in LPCAT1-deficient *rd11* mice, a new mouse model of retinal degeneration. We further proved an essential role of LPCAT1 in retinal photoreceptor degeneration and additional study is underway to clarify the detail mechanism of photoreceptor degeneration in *rd11* mice.

Acknowledgments

The authors thank Zibing Jin for assistance of rhodopsin staining in rods.

Supported by the National Natural Science Foundation of China (81371060), a retinal gene therapy study grant from Wenzhou Medical University, Wenzhou, China (QTJ11018), and National Institutes of Health (NIH) Grant EY023543.

Disclosure: **X. Dai**, None; **J. Han**, None; **Y. Qi**, None; **H. Zhang**, None; **L. Xiang**, None; **J. Lv**, None; **J. Li**, None; **W.-T. Deng**, None; **B. Chang**, None; **W.W. Hauswirth**, P; **J. Pang**, None

References

1. Hartong DT, Berson EL, Dryja TP. Retinitis pigmentosa. *Lancet*. 2006;368:1795–1809.
2. Pang JJ, Lei L, Dai X, et al. AAV-mediated gene therapy in mouse models of recessive retinal degeneration. *Curr Mol Med*. 2012;12:316–330.
3. Friedman JS, Chang B, Krauth DS, et al. Loss of lysophosphatidylcholine acyltransferase 1 (LPCAT1) leads to photoreceptor degeneration in *rd11* mice. *Proc Natl Acad Sci U S A*. 2010; 107:15523–15528.
4. Chen X, Hyatt BA, Mucenski ML, Mason RJ, Shannon JM. Identification and characterization of a lysophosphatidylcholine acyltransferase in alveolar type II cells. *Proc Natl Acad Sci U S A*. 2006;103:11724–11729.
5. Nakanishi H, Shindou H, Hishikawa D, et al. Cloning and characterization of mouse lung-type acyl-CoA:lysophosphatidylcholine acyltransferase 1 (LPCAT1). Expression in alveolar type II cells and possible involvement in surfactant production. *J Biol Chem*. 2006;281:20140–20147.
6. Pang JJ, Boye SE, Lei B, et al. Self-complementary AAV-mediated gene therapy restores cone function and prevents cone degeneration in two models of Rpe65 deficiency. *Gene Ther*. 2010;17:815–826.
7. Pang JJ, Dai X, Boye SE, et al. Long-term retinal function and structure rescue using capsid mutant AAV8 vector in the rd10 mouse, a model of recessive retinitis pigmentosa. *Mol Ther*. 2011;19:234–242.
8. Pang JJ, Deng WT, Dai X, et al. AAV-mediated cone rescue in a naturally occurring mouse model of CNGA3-achromatopsia. *PLoS One*. 2012;7:e35250.
9. Boye SE, Boye SL, Lewin AS, Hauswirth WW. A comprehensive review of retinal gene therapy. *Mol Ther*. 2013;21:509–519.
10. Zhong L, Zhao W, Wu J, et al. A dual role of EGFR protein tyrosine kinase signaling in ubiquitination of AAV2 capsids and viral second-strand DNA synthesis. *Mol Ther*. 2007;15:1323–1330.
11. Petrs-Silva H, Dinculescu A, Li Q, et al. Highefficiency transduction of the mouse retina by tyrosine-mutant AAV serotype vectors. *Mol Ther*. 2009;17:463–471.
12. Petrs-Silva H, Dinculescu A, Li Q, et al. Novel properties of tyrosine-mutant AAV2 vectors in the mouse retina. *Mol Ther*. 2011;19:293–301.
13. Haire SE, Pang J, Boye SL, et al. Light-driven cone arrestin translocation in cones of postnatal guanylate cyclase-1 knockout mouse retina treated with AAV-GC1. *Invest Ophthalmol Vis Sci*. 2006;47:3745–3753.
14. Hauswirth WW, Lewin AS, Zolotukhin S, Muzyczka N. Production and purification of recombinant adeno-associated virus. *Meth Enzymol*. 2000;316:743–761.
15. Pang JJ, Boye SL, Kumar A, et al. AAV-mediated gene therapy for retinal degeneration in the rd10 mouse containing a recessive PDEβ mutation. *Invest Ophthalmol Vis Sci*. 2008;49: 4278–4283.
16. Pang JJ, Cheng M, Stevenson D, Trousdale MD, Dorey CK, Blanks JC. Adenoviral-mediated gene transfer to retinal

Investigative Ophthalmology & Visual Science

explants during development and degeneration. *Exp Eye Res*. 2004;79:189–201.

17. Li W, Kong F, Li X, et al. Gene therapy following subretinal AAV5 vector delivery is not affected by a previous intravitreal AAV5 vector administration in the partner eye. *Mol Vis*. 2009; 15:267–275.
18. Li X, Li W, Dai X, et al. Gene therapy rescues cone structure and function in the 3-month-old rd12 mouse: a model for midcourse RPE65 leber congenital amaurosis. *Invest Ophthalmol Vis Sci*. 2011;52:7–15.
19. Zeng R, Zhang Y, Shi F, Kong F. A novel experimental mouse model of retinal detachment: complete functional and histologic recovery of the retina. *Invest Ophthalmol Vis Sci*. 2012;53:1685–1695.
20. Pang JJ, Chang B, Kumar A, et al. Gene therapy restores vision-dependent behavior as well as retinal structure and function in a mouse model of RPE65 Leber congenital amaurosis. *Mol Ther*. 2006;13:565–572.
21. Kong F, Li W, Li X, et al. Self-complementary AAV5 vector facilitates quicker transgene expression in photoreceptor and retinal pigment epithelial cells of normal mouse. *Exp Eye Res*. 2010;90:546–554.
22. Allocca M, Manfredi A, Iodice C, Di VU, Auricchio A. AAV-mediated gene replacement either alone or in combination with physical and pharmacological agents results in partial and transient protection from photoreceptor degeneration associated with beta PDE deficiency. *Invest Ophthalmol Vis Sci*. 2011;52:5713–5719.
23. Bainbridge JW, Smith AJ, Barker SS, et al. Effect of gene therapy on visual function in Leber's congenital amaurosis. *N Engl J Med*. 2008;358:2231–2239.
24. Maguire AM, Simonelli F, Pierce EA, et al. Safety and efficacy of gene transfer for Leber's congenital amaurosis. *N Engl J Med*. 2008;358:2240–2248.
25. Jacobson SG, Cideciyan AV, Ratnakaram R, et al. Gene therapy for leber congenital amaurosis caused by RPE65 mutations: safety and efficacy in 15 children and adults followed up to 3 years. *Arch Ophthalmol*. 2012;130:9–24.
26. Dalkara D, Byrne LC, Lee T, Hoffmann NV, Schaffer DV, Flannery JG. Enhanced gene delivery to the neonatal retina through systemic administration of tyrosine-mutated AAV9. *Gene Ther*. 2012;19:176–181.
27. Dalkara D, Byrne LC, Klimczak RR, et al. In vivo-directed evolution of a new adeno-associated virus for therapeutic outer retinal gene delivery from the vitreous. *Sci Transl Med*. 2013;5:189ra76.
28. Weltzien HU. Cytolytic and membrane-perturbing properties of lysophosphatidylcholine. *Biochim Biophys Acta*. 1979;559: 259–287.
29. Wilson-Ashworth HA, Judd AM, Law RM, et al. Formation of transient non-protein calcium pores by lysophospholipids in S49 lymphoma cells. *J Membr Biol*. 2004;200:25–33.
30. Tummala P, Mali RS, Guzman E, Zhang X, Mitton KP. Temporal ChIP-on-Chip of RNA-Polymerase-II to detect novel gene activation events during photoreceptor maturation. *Mol Vis*. 2010;16:252–271.
31. Mansilla F, da Costa KA, Wang S, et al. Lysophosphatidylcholine acyltransferase 1 (LPCAT1) overexpression in human colorectal cancer. *J Mol Med (Berl)*. 2009;87:85–97.
32. Zhou X, Lawrence TJ, He Z, Pound CR, Mao J, Bigler SA. The expression level of lysophosphatidylcholine acyltransferase 1 (LPCAT1) correlates to the progression of prostate cancer. *Exp Mol Pathol*. 2012;92:105–110.
33. Morita Y, Sakaguchi T, Ikegami K, et al. Lysophosphatidylcholine acyltransferase 1 altered phospholipid composition and regulated hepatoma progression. *J Hepatol*. 2013;59:292–299.
34. Bridges JP, Ikegami M, Brilli LL, Chen X, Mason RJ, Shannon JM. LPCAT1 regulates surfactant phospholipid synthesis and is required for transitioning to air breathing in mice. *J Clin Invest*. 2010;120:1736–1748.

Investigative Ophthalmology & Visual Science